

Structural and electronic properties of pentacene molecule and molecular pentacene solid

R. G. Endres,¹ C. Y. Fong,² L. H. Yang,³ G. Witte,⁴ and Ch. Wöll⁴

¹*Center for Computational Sciences and Computer Science & Mathematics Division, Oak Ridge National Laboratory, Oak Ridge, TN 37831-6114 USA*

²*Department of Physics, University of California, Davis, CA 95616-8677 USA*

³*H Division, Lawrence Livermore National Laboratory, Livermore, CA 94551 USA*

⁴*Lehrstuhl für Physikalische Chemie I, Ruhr-Universität Bochum, Universitätsstrasse 150, 44780 Bochum, Germany*

(Dated: November 26, 2024)

The structural and electronic properties of a single pentacene molecule and a pentacene molecular crystal, an organic semiconductor, are examined by a first-principles method based on the generalized gradient approximation of density functional theory. Calculations were carried out for a triclinic unit cell containing two pentacene molecules. The bandwidths of the valence and conduction bands which determine the charge migration mechanism are found to depend strongly on the crystallographic direction. Along the triclinic reciprocal lattice vectors \mathbf{A} and \mathbf{B} which are orientated approximately perpendicular to the molecular axes the maximal valence (conduction) band width amounts to only 75 (59) meV, even smaller values are obtained for the \mathbf{C} direction parallel to molecular axes even less. Along the stacking directions $\mathbf{A}+\mathbf{B}$ and $\mathbf{A}-\mathbf{B}$, however, the maximal valence (conduction) band width is found to reach 145 (260) meV. The value for the conduction band width is larger than estimates for the polaron binding energy but significantly smaller than recent results obtained by semiempirical methods. The single molecule has a HOMO-LUMO gap of about 1.1 eV as deduced from the Kohn-Sham eigenvalue differences. When using the self-consistent field method, which is expected to yield more reliable results, a value of 1.64 eV is obtained. The theoretical value for the band gap in the molecular solid amounts to 1.0 eV at the Γ -point.

I. INTRODUCTION

Organic semiconductors based on pentacene ($C_{22}H_{14}$) or other aromatic hydrocarbon molecules have recently attracted an enormous interest regarding their use for molecular electronics [1]. A pentacene field effect transistor showing a temperature-independent high-mobility ($\mu \sim 1.3 \text{ cm}^2/\text{Vs}$) has been fabricated[2]. It has to be noted, however, that in the latter case polycrystalline material was used; considerable higher mobilities can be expected for single crystalline material. Although mobilities for single crystalline pentacene have not yet been measured, recent work has demonstrated that epitaxial growth of pentacene on solid substrates may be possible [3], thus putting the realization of devices with an active layer of single-crystalline pentacene into sight. Despite this pronounced interest, however, there are still many open questions even on rather basic properties on molecular semiconductors like pentacene, in particular as far as the electronic structure is concerned. The conventional view is that in molecular crystals of aromatic molecules like pentacene hole transport is dominant and that the valence band width is of order 100 meV - much smaller than the experimental 500 meV estimate[4] for the conducting charge transfer salt TTF-TCNQ (tetrathiafulvalene-tetracyanoquinodimethane). The bandwidth is further important for understanding the charge transport mechanism. According to Holstein's polaron model[5], the small polaron limit (size of lattice constant) is reached when the electronic bandwidth is small compared to the polaron binding energy. The

binding energy is experimentally estimated to be of order ~ 200 meV[6]. On the theoretical side, however, there have only been very few reports. Using semiempirical methods, results ranging between $\sim 600 \text{ meV}$ obtained using the cluster approach with a semiempirical Hartree-Fock INDO (intermediate neglect of differential overlap)[7] and $\sim 120 \text{ meV}$ obtained from an extended-Hückel-type (EHT)-calculation[8] were reported.

In this paper, we address the above mentioned issues by using a first-principles algorithm [9]. In particular, we illustrate how the bandwidths of the VB and CB depend on the orientation of the herringbone structured crystal. We find that although there is only weak dispersion of the bands along the reciprocal lattice vectors \mathbf{A} , \mathbf{B} , and especially \mathbf{C} (along the molecules), along the stacking directions $\mathbf{A}+\mathbf{B}$ and $\mathbf{A}-\mathbf{B}$ the dispersion reaches significantly larger values. For these directions, the bandwidth of the CB and the next higher band CB+1 amounts to 149 and 260 meV. For the $\mathbf{A}-\mathbf{B}$ direction the VB and the next lower band VB-1 don't become quite as large, the corresponding values amount to 145 and 131 meV.

Hence, the band widths in the stacking directions can become larger than estimates for the polaron binding energy. This should make band-like transport at low temperatures possible. To the best of our knowledge this is the first fully *ab initio* bandstructure calculation and theoretical band gap estimate in the literature.

In section II, we discuss briefly the method of calculation. It will be followed by a section describing the models in section III. Results of the single molecule and the molecular solid and discussions will be presented in

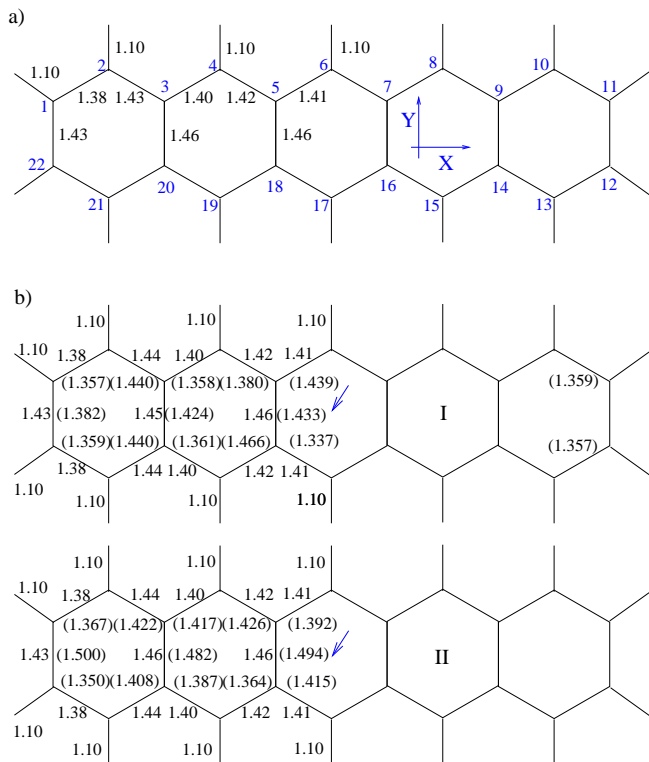


FIG. 1: Atomic bond-lengths a) of a fully relaxed single pentacene molecule (in xy -plane) and b) of the constrained relaxed pentacene crystal. One can clearly see the alternating double (shorter) and single (longer) bonds. The experimental values[16] are shown in brackets (...). The missing bond-lengths follow from symmetry.

section IV. Finally, in section V, a summary will be given.

II. METHODS OF CALCULATION

We used one of the popular density functional theory (DFT) algorithms with localized orbitals as the basis functions, SIESTA[10]. It uses Troullier-Martins norm-conserved pseudopotentials[11] in the Kleinman-Bylander separable form[12]. The basis set is made of pseudo atomic orbitals (PAO) of multiple-zeta form including optionally polarization orbitals. The first-zeta orbitals are obtained by the method of Sankey and Niklewski[13], while the second-zeta orbitals are constructed in the split-valency philosophy well known from quantum chemistry[14]. With this basis set, SIESTA calculates the self-consistent potential on a grid in real space. The fineness of this grid is determined in terms of an energy cutoff E_c in analogy to the energy cutoff when the basis set involves plane waves. In the present calculations, we used E_c to be 80 Ry and a double-zeta plus polarization orbitals (DZP) basis set. For the exchange-correlation energy functional, the generalized gradient approximation (GGA) in the version of Perdew-Burke-

Ernzerhof[15] is applied for characterizing semi-nonlocal effects.

III. MODELS

A. Single molecule

For the case of simulating a single molecule, we used a large cubic supercell ($50\text{\AA} \times 50\text{\AA} \times 50\text{\AA}$) and placed the molecule at the center. These dimensions are much larger than the pentacene dimensions ($14.21\text{\AA} \times 5.04\text{\AA}$ in x - y plane) and results in no interactions between the unit cells. The atoms in the molecule were relaxed until the magnitude of the force on each atom is less than the tolerance $0.04eV/\text{\AA}$.

B. Molecular solid

For the molecular solid, we used a triclinic unit cell containing two non-equivalent molecules. The unit cell data with the Bravais lattice vectors \mathbf{a} , \mathbf{b} (perpendicular molecular axes), and \mathbf{c} (along molecular axes) and atomic positions were taken from a previous x-ray measurement on a trichlorobenzene solution-grown single crystals by R. Campbell and co-workers (1961)[16]. The lattice vectors are $a = 7.93$, $b = 6.14$, $c = 16.03\text{\AA}$, $\alpha = 101.9$, $\beta = 112.6$, $\gamma = 5.8^\circ$. There are other structure determinations, e.g. by D. Holmes *et al.* (1999)[17]. Although the crystallization solvent was the same in both cases, the unit cell parameters disagree slightly. Their structure is similar to crystals obtained from the vapor-phase deposition technique which results in slightly denser molecular packing (unit cell volume reduced by 3%)[18]. Polymorphism is common in molecular crystals and depends on the applied preparation techniques and conditions[18]. The main structural features however are the same and we restrict ourselves to the analysis of pentacene crystal described by Campbell's data.

Since the GGA functional does not include van der Waals attraction[19, 20], we relaxed the atoms except 3 in each molecule in order to fix the planes of the molecules. The force tolerance is again $0.04eV/\text{\AA}$. The \mathbf{k} -point sampling is done just using the Γ -point. This is expected to be sufficient due to the large unit cell.

In \mathbf{k} -space, we denote the reciprocal lattice vectors \mathbf{A} , \mathbf{B} , and \mathbf{C} . We note however that the unit cell is triclinic and not tetragonal, although the unit cell angles are close to 90° . Hence by convention, e.g. \mathbf{A} is parallel to $\mathbf{b} \times \mathbf{c}$ but not to \mathbf{a} .

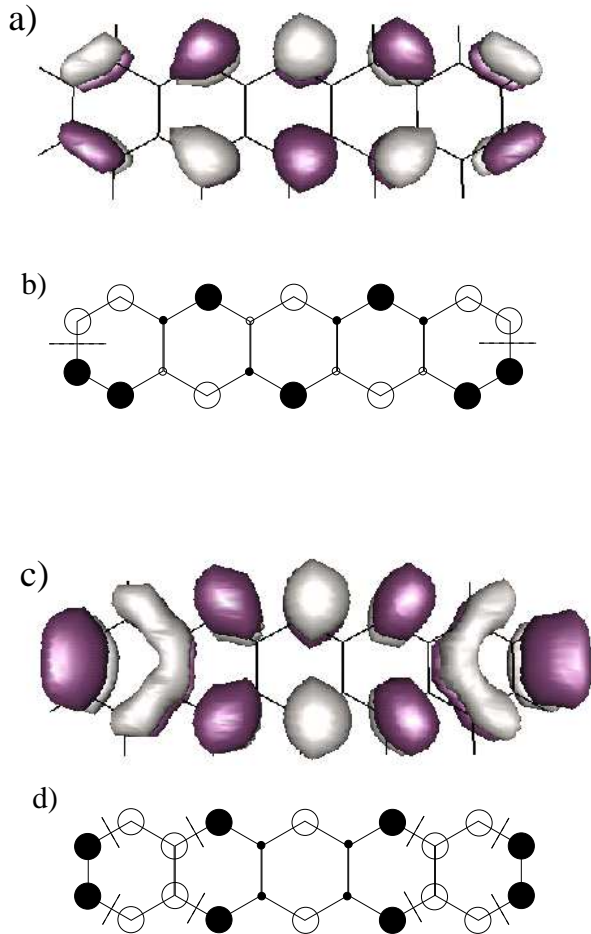


FIG. 2: Single particle wavefunctions of isolated pentacene molecule. The dark color represents a positive sign, the light color a negative sign. (a) and (b) show the HOMO, (c) and (d) the LUMO. (a) isosurface at $\pm 0.05/\text{\AA}^{3/2}$; (b) LCAO coefficients: small circles 0.01 - 0.09, large circles 0.12 - 0.3, the short lines show regions of high gradients; (c) isosurface at $\pm 0.03/\text{\AA}^{3/2}$, (d) similar to (b). Wavefunctions plotted with the program gOpenMol[24].

IV. RESULTS AND DISCUSSIONS

A. Single molecule

In figure 1 a) we show the relaxed single molecule. We label the atoms and give the bond-lengths. The z -coordinates for the relaxed atoms are less than $0.67m\text{\AA}$ about $z = 0$ showing that the molecule is essentially planar, in agreement with the experimental findings [17]. The molecule is symmetric with respect to the C atoms 6 and 17 and the midpoints of the bonds 1-22 and 11-12.

The bond-length in the y -direction is typically 1.46\AA , except at the ends where it is 1.43\AA . We will compare the C-C and C-H bond-lengths to experimental crystallographic data in section IV B. In general they are similar to those in graphite (1.42\AA). Our results show also smaller bond-lengths for the C atoms near the ends (bonds 1-2, 10-11, 12-13, and 21-22) to their respective neighbors along the x -direction. These bond-lengths are 1.38\AA . All the C-H bonds are 1.10\AA long.

The energy gap Δ separating the HOMO and the LUMO states is 1.1 eV as deduced from Kohn-Sham eigenvalue differences. This value is about 40% smaller than the experimental value, 1.82 eV, reported from ellipsometric spectra of thin pentacene films [21]. This underestimation of gaps by this magnitude is a common deficiency of the GGA functional [22]. Since DFT is a groundstate theory, better results can usually be obtained from total energy differences (self-consistent field method)[23]

$$\Delta = E_0(N) - E_0(N + 1), \quad (1)$$

where $E_0(N)$ is the groundstate of the neutral N (even) electron system and $E_0(N + 1)$ is the groundstate with one extra electron added in the same geometry as the neutral system. This gives a quantitatively better gap estimate of 1.64 eV.

The corresponding wave functions for these two states are shown in figure 2. Surprisingly, they are different from a previous calculation by Strohmaier *et al.* [25] using semiempirical MNDO (modified neglect of diatomic overlap). Their HOMO resembles our LUMO, while their LUMO has the same symmetries as our HOMO although contributions from carbon atoms near the end of the pentacene molecule seem different. We do not know the reason for the discrepancy. However, we checked our result further by comparing it to an elementary Hückel-type calculation only including the 22 p_z orbitals each contributing one electron. The signs of the wavefunction are the same as the ones obtained from the more elaborate SIESTA calculation.

Fig. 2 (a) shows the HOMO state. The main contribution to this wave function comes from the p_z orbital of the C atoms. In Fig. 2 (b), we show the coefficients of the wave function expanded onto the first-zeta basis functions which resemble most closely the atomic orbitals with p_z symmetry. The positive values are indicated by the filled circles and the negative values are shown by the open circles. The large circles correspond to a magnitude between 0.12 and 0.3, while the small circles represent a value between 0.01 and 0.09. Both figures clearly demonstrate that the C atoms contributing to the HOMO state are in a second neighbor (two large circles with a small circle in between) configuration near the center but in the nearest neighbor configuration at the two ends of the molecule. It is important to note that the relative phase of this molecular wave function varies by 180° in the nearest neighbor configurations at the ends of the molecule. In Fig. 2 (c), we plot the wave function of the LUMO

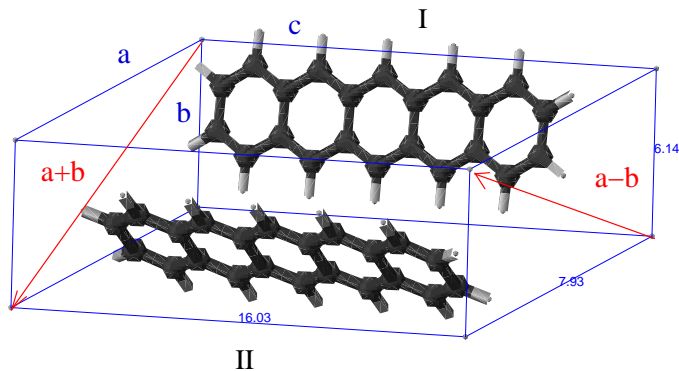


FIG. 3: Herringbone packing of two inequivalent pentacene molecules in the unit cell of Campbell's model. The molecules are relaxed although three atoms in each molecule are kept fixed. The Bravais lattice vectors \mathbf{a} , \mathbf{b} , and \mathbf{c} are assigned, as well as the vectors $\mathbf{a}+\mathbf{b}$ and $\mathbf{a}-\mathbf{b}$. Figure prepared with the program MOLMOL[26].

state. Similar to the HOMO state, the dominant contributing orbitals are also the p_z orbitals. As shown in Fig. 2 (d), similar second neighbor configuration near the center as in HOMO state is observed but there are more nearest neighbor configurations at the ends of the molecule. This difference at the ends of the molecule explains why the HOMO state has lower energy than the LUMO state because the latter state has a larger kinetic energy due to rapid (180°) phase changes.

B. Molecular solid

In figure 3 we show the structure for the molecular pentacene solid according to the results of Campbell. The triclinic unit cell for each case is depicted by thin solid lines. There are two molecules per unit cell labeled I and II following Campbell's notation which are not parallel to each other, but are packed in a herringbone fashion. The comparison of our atomic bond-lengths from the constrained relaxation with the experimental ones (in brackets) are shown in figure 1 b). The centers of symmetry of molecule I (0,0,0) and molecule II ($1/2, 1/2, 0$) in the space group P1 are marked by arrows. The two redundant bond-lengths at the right end of molecule I illustrate this symmetry. The bond-lengths are qualitatively correct and show the proper trends (alternating single-double bonds), but are in general slightly larger than the experimental ones as typical for the DFT method. Additionally, the experimental bond-lengths are not symmetric with respect to the long molecular axes as opposed

to the DFT result where the bonds are more symmetric similar to the single molecule (at least to this precision). This reflects that noncovalent bonding by nonlocal interactions is not treated properly. This deficiency however concerns mostly the total energy (and structure), less the single particle wavefunctions (and bandstructure).

The band structure along the high symmetry axes for energies ranging from -8 to -3.8 eV are depicted in figures 4 and 5. The bands always come in sets of two, due to the near degeneracy of the states of two pentacene molecules per unit cell. There are two important pieces of information one can read off the band structure plots.

First, we want to estimate the transfer integrals t between the two molecules in a unit cell and restrict ourselves to the couplings between the two HOMOs and between the two LUMOs. These are most important for the hole and electron transport, respectively. Since there is no momentum transfer involved for the intracell coupling, we can restrict ourselves to the Γ -point. At this point the bonding/antibonding splitting between two (identical) HOMO (LUMO) states is $2t_{H(L)}$. This gives $t_H = 85$ meV for the HOMO coupling and $t_L = 15$ meV for the LUMO coupling. Since the two molecules are in principle inequivalent where the level energy difference between the two HOMO (LUMO) states is $\Delta E_{H(L)}$, the true coupling $t'_{H(L)}$ follows from $2t'_{H(L)} = \sqrt{(2t_{H(L)})^2 - \Delta E_{H(L)}^2}$. This equation of a coupled inhomogeneous two level system was stated by Cornil *et al.*[7] (their Eq. (1)). In their work an offset energy $\Delta E_{H(L)}$ as large as 61 meV (70 meV) was quoted. While $\Delta E_H = 61$ meV leads to $t'_H = 80$ meV, $\Delta E_L = 70$ meV gives a negative discriminant, i.e. our t_L and Cornil's ΔE_L are not consistent. This at least illustrates that there cannot be a large offset in our case.

Second, the dispersion and bandwidth reflect the coupling between the unit cells and determines the crystal properties. The larger the bandwidth the more delocalized the electronic states are at finite temperature and the more one has transport by a band mechanism. If the bandwidth becomes small and comparable to the polaron binding energy, then excess charges are being self-trapped and need thermal activated to migrate by a hopping mechanism.

The bandwidths are shown in table I. At least along the triclinic reciprocal lattice vectors \mathbf{A} , \mathbf{B} , and \mathbf{C} they are all smaller than 73 meV and hence clearly smaller

[meV]	VB-1	VB	CB	CB+1
\mathbf{A}		73	29	
\mathbf{B}		62	59	
\mathbf{C}		23	25	
$\mathbf{A}+\mathbf{B}$	41	75	149	260
$\mathbf{A}-\mathbf{B}$	131	145	149	260

TABLE I: Bandwidths of valence band (VB), the next lower band (VB-1), the conduction band (CB), and the next higher band (CB+1) in meV.

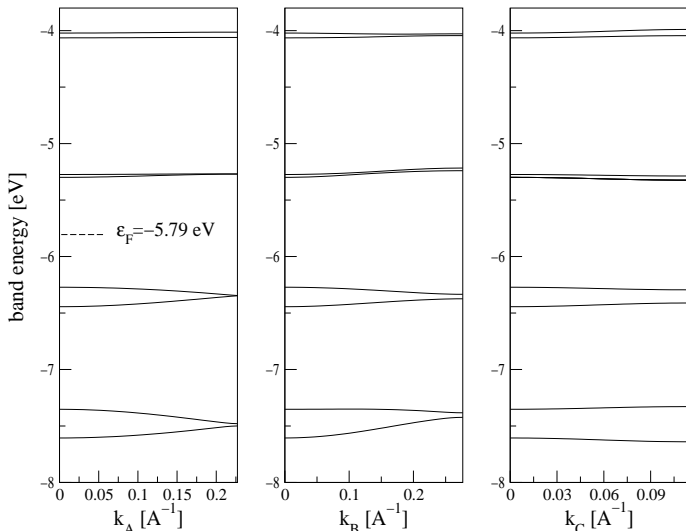


FIG. 4: Bandstructure along reciprocal lattice vectors **A**, **B**, and **C**. The LUMOs of the two molecules per unit cell couple less than the HOMOs, also the conduction band shows hardly any dispersion.

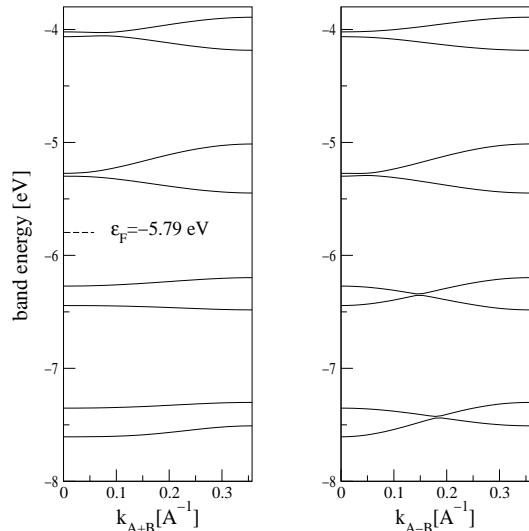


FIG. 5: Bandstructure along the stacking directions **A+B** and **A-B**. In these direction the bandwidths exceeds the polaron binding energy and band-like transport should be possible.

than estimates of polaron binding energies ($\sim 200\text{meV}$ [6]). This is likely to lead to a charge migration mechanism of some sort of hopping in these directions. Either the small polaron or the *multiple trapping and release* model [27] have been suggested. Our values for the bandwidths along **A**, **B**, and **C** are in semi-quantitative agreement with previous semiempirical ETH calculations by Haddon and co-workers[8].

It was suggested by Cornil and co-workers [7] using extrapolation of results from finite clusters that the bandwidth is much larger ($\sim 600\text{meV}$) in the stacking directions connecting the two inequivalent molecules. In

their Fig. 1, \mathbf{d}_1 connects the two molecules within same unit cell and \mathbf{d}_2 between neighboring unit cells. Here we calculated the bandstructure from first-principles along the high symmetry directions **A-B** and **A+B** resembling Cornil's \mathbf{d}_1 and \mathbf{d}_2 directions. We obtain that the width of the CB and in particular the next higher band CB+1 increases drastically to 149 and 260meV, respectively. On the other hand, we only observe an increase of the width of the VB and next lower band VB-1 in the **A-B** direction. At a first glance, they seem to be 211 and 247 meV. However, there is a band crossing for the two highest occupied bands. Since the triclinic unit cell has no symmetries (except the identity), the crossing bands mix and open a 10 meV gap (not resolved in plot). Due to the avoided crossing the widths of VB-1 and VB are only 131 and 145 meV, respectively.

If one assumes a cross-over between polaron-like and band-like transport at a bandwidth of 200 meV, band-like electron transport should be possible in the stacking directions. However, we do not observe bandwidths as large as those reported in Cornil's work [7]. When measuring the conductivity of a pentacene crystal or extracting the mobility from transistor characteristics, one should obtain thermally activated charge hopping as well as temperature-independent band transport behavior depending on the crystal orientation. Exactly this was observed by S. F. Nelson and co-workers (see their Fig. 3) [2].

The question whether the width of the CB is smaller or equal to the VB cannot be answered completely. Let us look at figure 4 first. The LUMO splitting and dispersion of the CB is clearly smaller than the HOMO splitting and dispersion of the VB. This in line with conventional expectations. On the other hand, figure 5 reveals that the bandwidths of the CB along **A+B** can indeed become larger than the VB bandwidth. In particular, the widths of CB+1 is drastically enlarged for **A+B** and **A-B**.

We further confirm by our method that there is hardly any dispersion in the **C** direction approximately along the pentacene molecules. As already pointed out in Ref. [7] this leads to a quasi 2-dimensional character for charge transport.

Finally, the fundamental band gap is 0.97 eV measured at the Γ -point. This is slightly smaller than the Kohn-Sham HOMO-LUMO gap for the single pentacene molecule, 1.10 eV, due to band offsets from Brillouin zone folding and bonding/antibonding splitting. As demonstrated in the case of a single pentacene molecule the gap is drastically underestimated.

V. SUMMARY

In conclusion, we used an ab-initio approach to determine the electronic properties and in particular the band-structure of a molecular solid of pentacene. A geometry optimization of the single molecule yields an essentially planar molecule in agreement with experiment.

The bond-lengths along the \mathbf{x} -direction (the direction of the molecule) do show 0.06\AA difference between the bonds at the ends and the middle of the molecule. Both the HOMO and LUMO states originate from the p_z orbitals on second neighbors C atoms in the center and on nearest neighbors C atoms at the two ends of the molecule. The relative phases and the extent of overlapping between the neighboring p_z orbitals differ for the two states.

For the solid pentacene, calculations we carried out using the first-principles tight-binding code SIESTA for a pentacene molecular crystal with the experimentally determined herringbone structure together with intramolecular distances resulting from a constrained geometry optimization. The resulting bond-lengths are in good agreement with experiment. The solid is predicted to be a large band-gap ($> 1.0\text{eV}$) semiconductor with an maximal bandwidth for electron transport of about 260 meV and a maximal bandwidth for hole transport of only 145 meV. It is found that the widths of the electronic bands depends strongly on the crystallographic direction. Along the triclinic reciprocal lattice vectors the

bandwidths are generally smaller than estimates based on the small polaron binding energy whereas. Along the stacking directions a significantly larger width is observed. The present maximum bandwidths are much smaller than previous results obtained using the semiempirical INDO approach. On the basis of the present theoretical results a band-like transport of charges in high-quality pentacene single crystal with very high mobilities should be possible at low temperatures, as previously observed experimentally for naphthalene[28].

Acknowledgement. We would like to thank P. Ordejón, E. Artacho, D. Sánchez-Portal and J. M. Soler for providing us with their *ab initio* code SIESTA. RGE thanks support from DOE-OS through BES-DMSE and OASCR-MICS under Contract No. DE-AC0500OR22725 with UT-Battelle LLC. CYF thanks the support of an NSF grant INT-987053, and NERSC at Lawrence Berkeley National Laboratory. LHY is supported by the DOE under contract number W-7405-ENG-48. CW and GW are funded by the Deutsche Forschungsgemeinschaft (OFET Grant No. Wo 464/17-1)).

-
- [1] G. Horowitz, *Adv. Mat.* **10**, 365 (1998), and references therein; J. Cornil, D. Beljonne, J. Ph. Calbert, and J. L. Brédas, *Adv. Mater.* **14**, 1053 (2001).
- [2] S. F. Nelson, Y. -Y. Lin, D. J. Gundlach, and T. N. Jackson, *Appl. Phys. Lett.* **72**, 1854 (1998).
- [3] S. Lukas, G. Witte, and Ch. Woll, *Phys. Rev. Lett.* **88**, 028301 (2002).
- [4] A. J. Heeger, in *Highly conducting one-dimensional solids*; J. T. Devreese, R. P. Evrard, V. E. van Doren, Eds. (Plenum Press, New York, 1979); p. 69 and references therein
- [5] T. Holstein, *Ann. Phys. (NY)* **8**,343 (1959).
- [6] A. R. Brown *et al.*, *Synth. Met.* **88**, 37 (1997).
- [7] J. Cornil, J. Ph. Calbert, and J. L. Brédas, *J. Am. Chem. Soc.* **123**, 1250 (2001); J. L. Brédas *et al.*, *Synth. Met.* **125**, 107 (2002).
- [8] R. C. Haddon *et al.*, *J. Phys. Chem B* **106**, 8288 (2002).
- [9] <http://www.uam.es/siesta>
- [10] D. Sánchez-Portal, P. Ordejón, E. Artacho, and J. M. Soler, *Int. J. Quantum Chem.* **65**, 453 (1997); E. Artacho, D. Sánchez-Portal, P. Ordejón, A. Garcia, and J. M. Soler, *Phys. Status solidi (b)* **215**, 809 (1999); P. Ordejón, E. Artacho, and J. M. Soler, *Phys. Rev. B* **53**, R10441 (1996).
- [11] N. Troullier and J. L. Martins, *Phys. Rev. B* **43**, 1993 (1991).
- [12] L. Kleinman and D. M. Bylander, *Phys. Rev. Lett.* **48**, 1425 (1982).
- [13] O. F. Sankey and D. J. Niklewski, *Phys. Rev. B* **40**, 3979 (1989).
- [14] S. Huzinaga, J. Andzelm, *et al.* ed "Gaussian basis sets for molecular calculations", Elsevier Science Pub. Co., New York, (1984).
- [15] J. P. Perdew, K. Burke, and M. Ernzerhof, *Phys. Rev. Lett.* **77**, 3865 (1996).
- [16] R. B. Campbell, J. Monteath Robertson and J. Trotter, *Acta Cryst.* **14**, 705 (1961).
- [17] D. Holmes, S. Kumaraswamy, A. J. Matzger, and K. Peter C. Vollhardt, *J. Euro. Chem.* **5**, 3399 (1999).
- [18] Th. Siegrist *et al.*, *Angew. Chem. Int. Ed.* **40**, 1732 (2001).
- [19] C. Adamo and V. Barone, *J. Chem. Phys.* **108**, 664 (1998).
- [20] S. A. Kafafi, *J. Phys. Chem. A* **102**, 10404 (1998).
- [21] S. P. Park, S. S. Kim, J. H. Kim, C. N. Whang, and S. Im, *Appl. Phys. Lett.* **80**, 2872 (2002).
- [22] W. Hanke and L. J. Sham, *Phys. Rev. Lett.* **43**, 387 (1979); M. S. Hybertsen and S. G. Louie, *Phys. Rev. Lett.* **55**, 1418 (1985).
- [23] R. O. Jones and O. Gunnarsson, *Rev. Mod. Phys.* **B 13**, 4274 (1989); C. J. Cramer and F. J. Dulles, *J. Am. Chem. Soc.* **116**, 9787 (1994).
- [24] L. Laaksonen, *J. Mol. Graph.* **10**, 33 (1992); D. L. Bergman, L. Laaksonen, and A. Laaksonen, *J. Mol. Graph.* **15**, 301 (1997). gOpenMol: A graphics program for the analysis and display of molecular dynamics trajectories.
- [25] R. Strohmaier, J. Petersen, B. Gompf, and W. Eisenmenger, *Surf. Sci.* **418**, 91 (1998).
- [26] R. Koradi, M. Billeter, and K. Wüthrich, K., *J. Mol. Graph.* **14**, 51 (1996). MOLMOL: a program for display and analysis of macromolecular structures
- [27] P. G. Le Comber, W. E. Spear, *Phys. Rev. Lett.* **25**, 509 (1970).
- [28] W. Warta, R. Stehle, N. Karl, *Appl. Phys. A* **36**, 163 (1985); N.Karl: "Charge-Carrier Mobility in Organic Crystals", in: *Organic Electronic Materials*, R. Farchioni and G. Grosso (eds.), Part II: Low Molecular Weight Organic Solids (chapter 8), (Springer Verlag, Berlin 2001)